Spring 5-2019

Potential Impact of Climate Change on the Distribution of Alpine Tundra in the Adirondack Mountains of New York

Terry Allard
University at Albany, State University of New York, tallard@albany.edu

Potential Impact of Climate Change on the Distribution of Alpine Tundra in the Adirondack Mountains of New York

An honors thesis presented to the
Department of Atmospheric and Environmental Sciences,
University at Albany, State University of New York
in partial fulfillment of the requirements for
graduation from The Honors College

Terence Allard

Research Advisor: Justin Minder, Ph.D.

May 2019

Abstract

Given the potential for significant changes in climate over the next century, understanding how biome locations may shift in response to these changes may be useful in informing conservation efforts. In this work the potential effect of climate change on the distribution of alpine tundra in the Adirondack Mountains of New York is examined. The ecological niche modelling software Maxent was used to analyze the distribution of alpine tundra relative to 30 year 800m PRISM climate normal data and terrain aspect over the Adirondacks. Random points from surveyed areas of alpine tundra in the Adirondacks were used as presence data in model training. The initial analysis was aimed at creating a model that was able to predict current alpine tundra distributions with a high level of skill. For the final analysis climate variables that contributed significantly to the skill of the model were downscaled to 10m resolution using an average lapse rate derived from the PRISM data. This analysis found that the presence of alpine tundra is well predicted by annual mean temperature. Different warming thresholds were applied to the climate grids and the model was rerun. The projected reduction in area of alpine tundra in the analysis area is calculated along with uncertainties in timing of area decline associated with different emission scenarios and GCM uncertainty.

Acknowledgements

I would like to thank:

My parents for their unyielding support of all my endeavors, and for instilling in me a love of the natural world that will stay with me always.

My research advisor Dr. Justin Minder, whose guidance, encouragement, and insight made this project possible.

Bill Hegman at Middlebury, for digging up the alpine tundra shapefiles that ended up being an incredibly useful resource!

All my friends here in Albany and back home, for all that you have done to support my development as a student, friend, and player of niche European board games over the last four years.

List of Figures

List of Tables

Table of Contents

Introduction

Alpine tundra ecosystems cover only around 3% of global land area and are found at latitudes ranging from near equatorial to near arctic; these isolated patches can contain samples of species not found in great abundance anywhere within hundreds or thousands of miles of their location (Körner, 2003). These patches can provide valuable information on the natural history of their region, and can be local hotspots of biodiversity (Körner, 1995). Alpine tundra ecosystems are typically defined as those that occur at an elevation exceeding the local treeline and having a community composition distinct from the surrounding forested lands (Gabriel & Talbot, 1984; Körner, 1998; Rundel & Millar, 2016). Alpine tundra communities are composed primarily of non-woody vascular plants, bryophytes and lichens whereas a forest community is dominated by woody plants over 3 meters in height (Gabriel & Talbot, 1984; Körner, 2007). There is some uncertainty and difficulty in precisely describing the location of the treeline on a given slope because of the gradual nature of the transition between densely forested areas and those that are treeless; one common way of delineating this transition is to use a line connecting the last large forested patches on the slope (Körner, 2007; Rundel & Millar, 2016).

There have been numerous efforts to find an environmental factor capable of accounting for this transition, many of which are described in the Alpine Treelines chapter of Körner (2003). Most of these efforts have found temperature-based climate variables such as mean growing season temperature, degree days above a threshold, and difference between summer and winter mean temperatures to be the best predictors of alpine tundra on a global or continental scale (Körner, 2003, 2004, 2007; Paulsen & Körner, 2014). Some research has suggested that the minimum root zone temperature for tissue growth in woody vascular plants may be significantly lower than the minimum temperature required for growth of non-woody vascular plant, lichens and bryophytes, therefore leading to the coldest regions on mountains being dominated by these non-woody plants (Körner, 1998). These analyses, along with many that have found significant changes in alpine tundra community composition and treeline elevation in the recent past associated with changes in temperature (Batllori et al. 2009; Danby, Koh, Hik, & Price, 2011; Gottfried et al. 2012; Jacobs, Chan, & Sutton, 2014; Silva et al. 2016) suggest that temperature is a good predictor of the transition between forest and alpine tundra at various scales of analysis. Studies have also documented changes in community composition in the alpine tundra communities across the North East United States in recent decades (Capers & Stone, 2011). A return to historic survey transects in the Adirondacks by Robinson et al. (2010) found that bryophytes and lichens went from constituting around 20% of area vegetation to around 10% from 1984 to 2007.

Given the previously observed impacts of warming temperatures on alpine tundra ecosystems and the near certainty for warming to occur globally over the next century (IPCC, 2007), understanding how future changes in climate could impact these regions may be useful in informing conservation efforts. There have been species distribution model analyses of the impact of a variety of climate change scenarios on alpine tundra in the European Alps finding that a 2 degree Celsius increase in temperature reduced alpine tundra area to an area about one quarter of its current size (Dirnböck, Dullinger & Grabherr, 2003).

An analysis of the impact of changing climate on alpine tundra like the one done by Dirnböck et al. (2003) has not yet been carried out on the Adirondack Mountains of New York. There are twenty peaks in the High Peaks region of the Adirondack Mountains that maintain communities of alpine tundra, these patches are among the southernmost in the Eastern United States and cover only about 26.3 ha or about 7 x 10^{-4} % of the Adirondack Park area (Carlson et al. 2011; Robinson et al., 2010). These alpine tundra patches have become a focus of major conservation efforts because they received significant damage through trampling and soil erosion from the large number of hikers in the region. Before the implementation of hiker education programs in the 1990’s, hikers were responsible for destruction of up to 30% of alpine tundra area on some peaks in the region (Ketchledge, 1977, 1979 as cited in Ketchledge, 1985). Recent surveys have found significant recovery in areas previously damaged by hikers in the region (Robinson et al., 2010). On some mountaintop transects, 50% of area that was bare substratum in 1984 transitioned to plant covered by 2007 (Robinson et al., 2010). Assuming the continued effectiveness of education and conservation efforts, direct physical damage to alpine tundra ecosystems from hikers should not significantly impact future alpine tundra presence in the region. In addition to this potential to be damaged by hikers, the alpine tundra of the Adirondacks may be sensitive to changes in climate. Because no previous attempts have been made to quantify the impact that warming may have on the alpine tundra of the Adirondacks, such an analysis could be provide insight on the temperature sensitivity of the community and potentially inform conservation efforts in the region.

Species distribution models can be used to make projections of how the distributions of species will change in altered environments (Elith et al., 2006). These models operate by finding a statistical relationship between species presence data and environmental predictors in a region (Elith et al., 2006). This statistical relationship can then be exposed to a new set of environmental variables, providing a probability of occurrence in this novel environment. However, uncertainty surrounding the true determining factors of the species distribution as well as the species ability to shift in response to changes in climate must be considered when applying these models to altered climate scenarios (Wiens et al., 2009).

The Maximum Entropy Software for Modeling Species Niches and Distributions (Maxent) was selected for use in this project because of its wide documented use in projecting species distributions in future climates and evidence suggesting it is able to outperform many other species distribution models in standardized tests (Elith et al., 2006; Phillips et al., 2017a). Developed in the early 2000's, Maxent was made to integrate more advanced machine learning techniques into the field of species distribution modelling and offer improved performance over other software available at the time (Elith et al., 2006; Phillips, Dudik, & Schapire, 2004). Maxent is a presence-only model, meaning that the only information that is provided by the user about species distribution is where occurrences have been observed (Phillips et al., 2004). Other niche-modelling software such as DesktopGarp and S-Plus also use absence data which can be difficult to acquire an accurate set of for many species (Elith et al., 2006).

Maxent estimates the distribution of the species across the landscape by finding the distribution function that maximizes entropy (is as close to a uniform distribution as possible) while still within the bounds of information given by the user-provided species presence data (Phillips, Dudik, & Schapire, 2004). For each environmental variable a set of features are created; a feature, denoted f_j is a function describing how the environmental variable is distributed across the analysis region (Elith et al., 2010). These features can be based on a single environmental variable, the square of a single variable, a threshold of a single variable, or the product of two variables (Elith et al., 2010; Phillips & Dudík, 2008). Each of these features is used for calculating a characteristic of the species distribution (Table 1). These features are then combined as a linear combination in the exponent of a Gibbs distribution to generate the estimator $\hat{z}$. The estimator $\hat{z}$ is a probability density function that approximates the true distribution of the species denoted Z, another probability density function (Phillips, Dudik, & Schapire, 2004). This approximation of Z is informed by the distribution of the species presence data provided by the user denoted z^*

(Phillips, Dudik, & Schapire, 2004). The first step in the process of generating $\hat{z}$ is finding all $\hat{z}$ such that the $E(\hat{z}(f_j)) = E(z^*(f_j))$ for all features, where the function $E()$ denotes expected value (Phillips, Dudik, & Schapire, 2004). It is possible that many different probability density functions will meet this criterion, so the distribution with maximal entropy (closest to uniform distribution) is selected (Phillips, Dudik, & Schapire, 2004; Phillips & Dudík, 2008). Once a satisfactory estimator $\hat{z}$ is created, the software outputs species probability across the region, the relative weights of each feature used, and optionally, an analysis of how much each environmental variable contributed to the skill of the model (Phillips, Dudik, & Schapire, 2004; Phillips & Dudík, 2008). This process is capable of generating accurate predictions of species presence across a variety of taxa, landscapes, and scales of analysis (Elith et al., 2010).

Methods

In this analysis Maxent models were run using a variety of climate variables to identify a set that could be used to predict alpine tundra presence skillfully in the analysis region. The initial climate dataset used was at too coarse a resolution for analysis beyond initial variable testing, so annual average temperature and precipitation values were downscaled to 10m from another nationwide climate dataset and used as climate input for further Maxent models. Maxent models were built using downscaled climate data and terrain aspect to determine if aspect would contribute to model skill. Finally, the model using downscaled annual average temperature and precipitation was used to make a projection of the potential impact of various degrees of warming from 0.25C to 2.0C on the area of alpine tundra found in the Adirondacks.

Initially an attempt was made to acquire species specific presence location data for a large number of Adirondack alpine tundra species listed as being present in Robinson et al.

(2010). After an extensive search the only potential source we found for such data was the species specific climate model resource on the Canadian Department of Natural Resources' plant hardiness website (Natural Resources Canada, 2017). A request for the species location data described on the website was denied because of established data sharing agreements (D. McKenney, personal communication). As an alternative, data from a previously conducted field survey of Adirondack alpine tundra patches conducted by Carlson et al. (2011) were used as the presence input for Maxent. This survey produced outlines of patches on all twenty peaks with alpine tundra by collecting coordinates around the perimeter of patches using handheld GPS devices (Carlson et al. 2011). The maximum amount of horizontal error for any patch was 3m, and Carlson et al. (2011) describe that most patches had "much less" error. The shapefile of the alpine tundra patches, and all other geospatial files used throughout this project were projected to the geographic coordinate system associated with North American Datum 1983. The random point generator tool in the open source GIS software QGIS was used to create a collection of points within the perimeter of the surveyed patch shapefile. For the initial Maxent model using 400m resolution data 100 points were created. For the models run on 10m grids 2500 points were used. In both cases the goal was to ensure that almost all grid cells under tundra patches contained a point. These points were used as the presence data input for the Maxent model. These points were converted from their native format to .csv format and arranged in Microsoft Excel to meet the formatting requirements of Maxent.

The climate data used in our initial analysis came from the Bioclimatic Predictors for Supporting Ecological Applications in the Conterminous United States dataset, found online under the name United States Geological Survey (USGS) Data Series 691 (USGS, 2012). These bioclimatic predictors are based on annual and monthly Parameter-elevation Regressions on Independent Slopes Model (PRISM) climate normal data at 800m and 4000m spatial resolution that have been downscaled to 400m and parsed into a variety of variables that have been found to be relevant biological distributions (Daly et al., 2008; USGS, 2012) (Table 2). The PRISM climate dataset incorporates quality controlled temperature and precipitation data from around 10,000 stations nationwide and a regression of climate and elevation to estimate the climate normal state across the entire United States from 1981- 2010 (Daly et al., 2008). A variety of factors including station proximity to coastline, and elevation are used in weighting stations for their contribution to the estimate of climate for a given location (Daly et al., 2008).

An initial Maxent analysis was run incorporating all twenty USGS bioclimatic predictors as environmental variables and 100 alpine tundra points as presence data. The jackknife analysis from this model was used to find the predictors that contributed most to the skill of the model and informed predictor selection in future model runs (Figure 1). Because of the small size of alpine tundra patches in the analysis region and the inability of the 400m USGS dataset to resolve individual patches, it was concluded that significant further downscaling would be necessary to accurately represent the current climate state for model building. By training a model on climate data that more accurately represented the current climate state, more accurate predictions of the response of alpine tundra to changes in climate would be made.

The downscaling process involved several steps to bring the 800m climate data to 10m resolution. The first step was resampling all rasters to the resolution of the high-resolution DEM. A single rate of change of the climate variable with respect to elevation, called a lapse rate was found for each variable across the analysis region. The lapse rate was calculated through a linear regression of the variables with respect to elevation. The slope of the line of best fit from this linear regression was used as the lapse rate across the region for that variable. These lapse rates were multiplied by the difference in elevation between the coarse resolution DEM and the finer resolution DEM, and the change in variable value was then added to the resampled variable raster to generate the final downscaled raster.

To identify potential candidates for this downscaling, a linear regression of all twenty USGS bioclimatic predictors with respect to elevation was performed. The results of this linear regression are listed in Table 3. An R^2 value near 1 in this regression suggests that the line of best fit is a good approximation of the elevation dependence of the variable for a wide range of elevations found in the region, and the variable is therefore a good candidate for downscaling using a single lapse rate.

A visual analysis of various raster resolutions relative to alpine tundra patch size led to the conclusion that downscaling to a grid size of approximately 10m x 10m would provide sufficient resolution for the analysis. At this resolution, most alpine tundra patches are resolved with several pixels. The USGS 1/3 arc second (approximately 10m x 10m) DEM product was selected as the elevation dataset for this downscaling. These files were downloaded from the USGS National Map website (TNM Download, 2019). A single DEM file from this dataset did not cover the entire analysis region, so the four DEMs listed in Table 4 were merged in ArcMap using the Mosaic to New Raster tool with pixel type set to “32 bit signed” to produce a single DEM that covered the entire analysis region. This merged DEM was then clipped to the analysis region using the Raster Clip tool in ArcMap.

PRISM 30-year 800m climate normals were selected as the source for climate data for subsequent analyses. The 800m PRISM normals were downscaled to a resolution of 10m; at this resolution most patches of alpine tundra had multiple grid cells covering them. To perform this downscaling monthly climate normals for mean temperature and mean precipitation along with elevation were acquired from the PRISM website at a resolution of 800m (PRISM Climate Group, 2015). The rasters were clipped to the area of the analysis region using the Raster Clip tool in ArcMap. A linear regression of mean temperature and of mean precipitation was performed relative to elevation for each month on this clipped dataset. The slope of the regression line was later used as the average lapse rate for the predictor in that month in the analysis region (Table 5). For temperature, the lapse rates varied from 3.5C/km to 6.0C/km and had lapse rates above 0.61 for all months and above 0.85 in all non-winter months. The values of lapse rate for precipitation varied from -36mm/km to -57 and had R^2 values above 0.5 for 5 of the months.

The clipped 800m PRISM dataset was resampled to the same resolution as the USGS 1/3 arc second DEM using the Resample tool in ArcMap. Bilinear interpolation resampling was used to avoid aliasing that would occur with nearest neighbor interpolation. The DEM was set as the snap raster under the environmental settings for all resampling operations to ensure that pixels were properly aligned for use in Maxent. Once all the monthly datasets were resampled, the Raster Calculator tool in ArcMap was used to apply the lapse rate from the linear regression to each of the monthly datasets using the following equation.

Equation 1.)

$$P_{new} = P_0 + (\Delta elevation)(\Gamma_P)$$

P_{new} = new predictor value; P_0 = Initial predictor value; Γ_P = predictor lapse rate

Δelevation = Elevation difference between 10m DEM and resampled PRISM elevation

The annual mean of the downscaled monthly predictors was calculated using the raster calculator tool and used as the annual average for that climate variable. These annual average rasters were exported as ASCII files using the Raster to ASCII tool in ArcMap for use in Maxent.

Terrain aspect was also considered as a model training predictor because of evidence that alpine tundra is more prevalent at some aspect values than others in the analysis region and other locations in North America (Carlson et al., 2011, Danby et al., 2011). Terrain aspect data was generated from the 1/3 arc second USGS DEM using the Aspect tool in ArcMap. Aspect data were converted to a categorical format using nested conditional statements in the Raster Calculator tool of ArcMap. This categorical raster was exported as an ASCII file using the same procedure as the annual average climate predictors. Preliminary Maxent models were run to determine the relative importance of the selected environmental predictors and to ensure that the model was highly skilled at predicting alpine tundra presence under climate normal conditions (Table 6, TPA-1, TPA-2, TP-1).

To simulate potential climate change scenarios a constant value was added to every pixel of the annual average temperature raster; this process was carried out using several different constant values ranging from 0 to 2 degrees Celsius at 0.25 degree increments. Maxent was run for the final climate impact analysis using the projection option which allows users to input environmental predictors with altered values; Maxent then provides as an output probability of occurrence in the new climate (Phillips, 2017). To correct for the overestimation of presence in the model, a ratio of true area to predicted area was calculated from the climate normal model (Table 6, TP-1) and used as a correction factor for predicted area in the current climate and in climate projection models.

The Maxent software provides several useful metrics for analyzing the distribution of species across the analysis landscape, the general skill of the model at predicting presence, and the relative contribution of each variable to model skill. For analyzing predicted presence across the analysis region, a map with probability of presence values is produced. These maps can be used to calculate area of predicted presence above a threshold and analyze changes in distribution for different climate scenarios. To measure the relative skill of the model Area under the ROC curve (AUC) is used. AUC is the sum of the probabilities of randomly chosen species presence locations having higher values for probability of occurrence than a randomly chosen background point (Swets, 1998). The closer the AUC value is to 1 the more skilled the model is considered (Swets, 1998).The relative importance of the environmental variables is conducted through an analysis of variable contributions (Phillips et al., 2017). Two values are given to the user from his analysis. The first value is called percent contribution, it represents the amount of prediction skill as measured by AUC that came from that variable (Phillips et al., 2017). The second analysis randomly changes the values of the environmental variable across the analysis region and records the amount of model skill lost as measured by AUC (Phillips et al., 2017). This loss in skill is used to calculate the relative importance of that variable. The Jackknife analysis shows how skilled the model would be if it were to be run either exclusively with a certain variable, or run excluding the variable (Phillips et al., 2017). Additionally, for each variable a response curve showing how the probability of occurrence relative to the range of values that variable takes on is produced. Another way of analyzing the contribution of each environmental variable is to analyze the .lambdas file that is produced with every Maxent run. This file contains information on what features were in the model. The lambda value for a feature tells how much weight that feature was given, as described in the introduction section. These metrics are examined for each of the Maxent models run for this project to gain insight into their operation and skill of prediction.

Results

The initial Maxent analysis using the USGS bioclimatic variables as environmental layer inputs (Table 6; BC-1) yielded results that were used to inform the decision of what variables to include in the final analysis. The AUC of the model was 0.998, suggesting the model was highly skilled at predicating alpine tundra presence (Table 7). The Jackknife analysis (Figure 1) found that the variables that were most skilled at predicting the presence of alpine tundra by themselves were: annual mean temperature, minimum temperature of coldest month, mean temperature of warmest quarter, and mean temperature of coldest quarter. The analysis of variable contributions should be considered a result of secondary importance to the jackknife when analyzing results because of issues that arise when environmental variables are highly correlated. This analysis of variable contribution found that mean temperature of driest quarter and mean temperature of coldest quarter were found to have the largest contribution to model skill, and altering minimum temperature of coldest month was found to cause the largest loss in model skill (Table 8). This is consistent with analyses that have previously analyzed trends connecting climatic variables and alpine tundra location (Körner, 2003, 2004, 2007; Paulsen & Körner, 2014). Precipitation variables were found have a minimal contribution to the skill of the model (Figure 1).

Because this model suggested that various temperature variables contributed significantly model skill and were skilled at predicting alpine tundra presence by themselves, annual average temperature was chosen for further analysis. Despite the relatively low skill of the precipitation variables (Figure 1), annual average precipitation was included because of its importance as a predictor in species distribution models run for alpine tundra species in the European Alps (Dirnböck, Dullinger & Grabherr, 2003). As previously discussed, downscaling to significantly finer resolutions was also deemed necessary for further analysis based on visual analysis, and the fact that the alpine tundra patches on some mountains are less than 10 meters across (Carlson et al., 2011). The finest resolution dataset available for the entire analysis region was the USGS 1/3 arc second (approximately 10m x 10m) DEM (USGS CITE). This DEM was used in the downscaling analysis and is therefore the resolution of the climate data used in the final analysis.

The next model (Table 6, TP-1) was made to determine if using only downscaled values of annual mean temperature and annual mean precipitation would generate a model as skilled as the one that used all twenty bioclimatic variables. The AUC from this analysis was 0.996. This is very close to the AUC of model run BC-1, suggesting that the two models have similar skill at predicting the presence of alpine tundra (Table 7). The contents of the lambdas file presented in Table 9 show that this two-variable model incorporates a large number of forward hinge features based on annual average temperature and incorporates few features based on annual average precipitation. The large number of temperature forward hinge variables, and their relatively large lambda values (compared to the precipitation hinge feature) suggests that the model was resolving a linear decrease in alpine tundra presence with decreasing temperature, and giving these features a relatively large weight in the final model. The large difference between the ‘with only’ and ‘without’ from the jackknife analysis in Figure 2 shows that annual average temperature is responsible for the majority of the skill in this model. When the model is run using only temperature as an input model skill is very nearly the same as when it is run with both variables. When the model is run without temperature data, the skill of the model is drastically decreased.

The next set of models were made to determine if incorporating terrain aspect would contribute significantly to model skill and to determine if product features combining aspect with one of the climate variables would be created. The alpine tundra patches in the Adirondacks are not evenly distributed across all different values of aspect, there is about 25% more area on east facing slopes than on any others (Carlson et al., 2011). Aspect was analyzed in two forms in two Maxent runs, first including values from across the entire analysis region (TPA-1) and then only including values from elevations above 1000m (TPA-2). The AUC values for TPA-1 and TPA-2 were both 0.995 (Table 7), this value very close to the AUC of TP-1 suggesting all models were similarly skilled. The response curve for alpine tundra to aspect is essentially flat for both the masked and unmasked analysis meaning that the different categories of aspect had the same probability of alpine tundra occurrence across them (Figure 3, Figure 4). The jackknife analyses show that a model using aspect alone is not skilled at predicting presence, and that removing aspect does not remove skill from the model (Figure 5, Figure 6). The lambdas file from TPA-1 and TPA-2 do not contain any instances of product features incorporating aspect into them suggesting that covariance between aspect and the climate variables was not an important factor (Table 10, Table 11). Because of the results showing that aspect did not contribute significantly to the skill of the model it was not used in further model runs.

The final analysis attempts to make a projection of how changes in temperature associated with global climate change could potentially impact the distribution and area of alpine tundra in the region. Model TP-1 was used in this analysis because it was found to be as skilled as BC-1, TPA-1, and TPA-2 while providing higher resolution results than BC-1 and being less computationally intensive than TPA-1 or TPA-2. There were very slight variations in the lambdas file output between this second running of TP-1 and the initial run because of the random nature of training point and background point selection by Maxent. The model was exposed to climate data with temperature increases ranging from 0 to 2 degree C at 0.25 degree intervals. The predicted area of alpine tundra is shown to decay exponentially as warming amounts increase (Figure 7, Figure 8). The nature of this decay comes from the decreasing surface area of the mountains with elevation. The surface area of a roughly conic mountain above an elevation contour will decay exponentially as that contour is moved up the mountain. Because the alpine tundra presence is well predicted by colder temperatures, and temperatures are decreasing with elevation, the contour representing the 70% likelihood of alpine tundra moves upslope with warming temperatures and encompasses a surface area that is decaying exponentially as it climbs. Approximately half of alpine tundra area is predicted to be lost at 0.25C of warming, 75% of area at 0.5C of warming and 100% between 1.25 and 1.5C of warming. These are all lower than the amount of warming projected to occur by the year 2050 in the North Eastern United States by the USGCRP under scenario RCP 4.5 (USGCRP, 2017).

Conclusion & Discussion

When interpreting these results, it must be noted that the timeframe of the RCP scenarios used in Figures 7 and 8 do not represent the timeframe at which changes in the area of alpine tundra are predicted to be observed. Plants in high elevation environments do not respond in a single season to changes in their environment; it may take years or decades for changes in distribution or community composition to be observed (Grabherr et al., 1994). Additionally, once these changes begins to occur they likely will not be at a high rate. It is estimated that most plant species are only capable of shifting their range upslope at 5 to 10 m per decade (Chen et al 2011) and changes in community composition often take decades to occur (Batllori et al. 2009; Gottfried et al., 2012; Robinson et al., 2010).

The estimated amount of warming required to reduce the area of the Adirondacks that is climatically suitable for alpine tundra by 75 to 100% is lower than the amount of warming that has been estimated for a similar reduction in other parts of the world. For instance, in the Calcareous Alps near Vienna, Austria it has been projected that a warming of 2 Degrees Celsius would cause the area of alpine tundra in the region to be reduced to an area about one quarter of its current size (Dirnböck, Dullinger & Grabherr, 2003). Projections of alpine tundra in Scotland suggest that a warming of 1.7C would lead to 70% of alpine tundra plants in the region losing all of their suitable climate area and a warming of 3.3C would lead to 80% of species experiencing a total loss of suitable climate area (Schneiderbauer et al., 2011). Projections over the Qinghai Province of China that suggest a warming of 1 to 3 Degrees Celsius would be enough to a make around three quarters of current alpine tundra become dominated by forest communities (Zhang et al., 2010).

The difference in the amount of warming required for 75 -100% reduction in suitable alpine tundra area for these projections and our projection in the Adirondacks may be explained by difference between the regions. The alpine tundra in the Adirondacks totals only about 65 acres and is found only within a roughly 400m elevation range (Carlson et al. 2011) while the area of alpine tundra in the other analysis regions cover hundreds or thousands of acres and is found in an elevation range of over 1000m (Dirnböck, Dullinger & Grabherr, 2003; Schneiderbauer et al. 2011; Zhang, 2010). Because the alpine tundra presence is connected to colder temperatures, and temperatures generally decrease with elevation, locations with a greater range of elevation suitable for alpine tundra will have more area for species to retreat to as warming occurs, thus allowing for more warming before all suitable habitat is lost.

There were several assumptions made in the methods of our projection that should be taken into consideration when analyzing the results. The assumption of a uniform warming of the region with no variations around features like elevation is may not be representative of reality (Pepin et al., 2015). It is not clear if this assumption of uniform warming overestimates warming in Adirondack peaks or underestimates it. There is evidence that higher elevations locations a few hundred miles from the Adirondacks on Mt. Washington in New Hampshire experienced a smaller magnitude of climate change than surrounding low elevation locations from 1930 to 2006, possibly because of thermal inversions and frequent cloud fog near the summit (Seidel et al., 2009). However, it is not clear if this trend is representative of other mountains in the region (Seidel et al., 2009). Conversely, Wilson and Nilsson (2009) found that the amount of change in bioclimatic temperature variables in alpine tundra zones in the Alps was about four times larger than in the surrounding lowlands over 30 years from 1987 to 2007. Depending on the relationship between elevation and magnitude of warming in the high elevation locations in the Adirondacks, the temperatures suitable for alpine tundra to occur at may cease to exist at a time that is sooner, or later than the one predicted by the RCP scenarios.

There are also potential sources of error in the climate data used in the Maxent models. This error stems from the lack of high-elevation temperature and precipitation monitoring stations across the Adirondacks in the PRISM dataset and in the downscaling process used to further downscale PRISM data used in this analysis. In the PRISM dataset, the climate normals at high elevation locations are estimated using values from nearby monitoring stations that are located at much lower elevations than the mountain peaks that contain alpine tundra. This lack of data measured directly at the site of alpine tundra leads to uncertainty about the true climate normal conditions at these locations. The assumption of a constant lapse rate across the entire region made in this analysis is likely not representative of reality; large topographic features can lead to spatial variations in lapse rate across a region (Minder, Mote, & Lundquist, 2010). Variations in lapse rate across the analyses region could mean that the climate data used in the Maxent models is significantly different than reality.

Another major assumption is that the alpine tundra species of the Adirondacks will respond uniformly to changes in climate. Performing a Maxent analysis on the alpine tundra community as a whole does not allow models to project the ways in which the community composition could change as a result of increases in temperature, or the sensitivity of individual species to warming. As mentioned earlier, there is evidence that warming temperatures cause tundra ecosystems to shift towards containing fewer lichens and bryophytes, and more vascular plants (Batllori et al. 2009; Gottfried et al. 2012; Silva et al. 2016, Jacobs, Chan, & Sutton, 2014; Danby, Koh, Hik, & Price, 2011). These changes in community composition and shifts in individual species ranges could be more informative than looking at all species of the alpine tundra together as a single unit. In order to have a sufficiently large amount of location data, presence locations would likely need to be included from locations across the eastern US and Canada, not just the Adirondacks. Presence data from a wide geographic extent would also serve to represent the range of climate that the species are capable of living in more accurately than only using data from the Adirondacks.

If a dataset was found that included reliable species-specific location data across a wide extent a similar Maxent modelling approach to the one used in this paper could be used. Because of the inclusion of international presence locations, the USGS Bioclimatic dataset could not be used as environmental input. It would likely be necessary to use an international bioclimatic dataset such as WorldClim (Fick & Hijmans, 2017) or other data source for bioclimatic variables across N. America at sufficiently high resolution. The difficulty in this approach would be in downscaling the coarse international climate data to a resolution capable of representing the Adirondack region accurately. The finest resolution available from the WorldClim dataset is 30 arc second or approximately 900m x 900m (Fick & Hijmans, 2017). Downscaling climate variables to a level capable of resolving alpine tundra patches for a region that spans hundreds or thousands of miles and then running a Maxent model over these variables would require a tremendous amount of computational resources. This kind of analysis would, however provide a more accurate representation of how the Adirondack alpine tundra community may respond to changes in climate, and allow for analysis of alpine tundra sensitivity to climate change at locations across the Eastern United States and Canada.

It is also possible that variables like icing and wind that are not included in the USGS or PRISM datasets may be responsible for the distribution of alpine tundra in the Adirondacks. Carlson et al. (2011) found that mean patch elevation on mountain was strongly correlated ($R^2 > 0.96$) with the elevation of the mountain itself. On all peaks that they surveyed, patches of alpine tundra were within about 75 meters of the top of the mountain (Carlson et al., 2011). Because patches of alpine tundra on the highest peaks are not extending hundreds of meters to elevations (and temperatures) that support alpine tundra on other lower peaks, it is possible that a variable other than temperature may be causing the patch distribution we see. Factors like riming, and wind desiccation may be more prevalent at the tops of these prominent peaks, and may be the ultimate cause of the distribution that is observed.

The overall goal of this analysis was to make projections of how alpine tundra distribution in the Adirondacks could change in a variety of climate change scenarios through Maxent modelling with downscaled climate data and presence location data from the region. Similar projections have been made for several regions of alpine tundra around the globe, but had not yet been carried out in the Adirondacks. Understanding how this community may respond to warming could be informative for efforts to preserve its presence in the region. To perform this projection, Maxent models were first run using a variety of climate variables to identify a set that could be used to skillfully predict alpine tundra presence in the region under climate normal conditions. Annual mean temperature and precipitation were identified as the variables to be used in the projection.

The PRISM datasets for monthly average temperature and precipitation were at 800m resolution. This was too coarse to resolve the patches of alpine tundra in the area. The monthly PRISM datasets were downscaled to a resolution of approximately 10m using a lapse rate derived from a linear regression of elevation and monthly values. These downscaled monthly datasets were averaged to create annual average values. Test models including terrain aspect found that it did not contribute to model skill, and was therefore not used in projection analyses.

A Maxent model based on annual average temperature and precipitation projection was used to determine the impact of warming between 0.25C and 2.0C on alpine tundra distribution. One half of alpine tundra area was projected to be lost at 0.35C of warming, three quarters of area lost at 0.5C and all area lost between 1.25 and 1.5C. These values are all lower than the USGCRP projection for warming in the North East United states by the year 2050 under warming scenario 4.5 (USGCRP, 2017). It should be noted that the change in area should not be expected to occur in the same timespan as the warming. Changes in community composition, and community location can take decades to occur (Batllori et al., 2009; Gottfried et al., 2012; Robinson et al., 2010).

Several of the underlying assumptions of the methods used lead to uncertainty in the model results. These include the lack of information on community composition change, the potential for factors like wind and icing to influence alpine tundra distributions, and the assumption of uniform warming and lapse rate across the region. Overall, these results suggest that the alpine tundra of the Adirondacks may be sensitive to changes in temperature that are nearly certain to occur in the next century. Further research incorporating species specific models, and variables such as rime ice accumulation and wind may provide more accurate results on the true impact that climate change could have on the region.

References

Batllori, E., Blanco-Moreno, J., Ninot, J., Gutiérrez, E., & Carrillo, E. (2009). Vegetation patterns at the alpine treeline ecotone: The influence of tree cover on abrupt change in species composition of alpine communities. *Journal of Vegetation Science, 20*(5), 814-825. doi: 10.1111/j.1654-1103.2009.01085.x

Capers, R., & Stone, A. (2011). After 33 years, trees more frequent and shrubs more abundant in Northeast U.S. alpine community. *Arctic, Antarctic, and Alpine Research, 43*(4), 495-502. doi: 10.1657/1938-4246-43.4.495

Carlson, B., Munroe, J., & Hegman, B. (2011). Distribution of alpine tundra in the Adirondack Mountains of New York, U.S.A. *Arctic, Antarctic, And Alpine Research, 43*(3), 331-342. doi: 10.1657/1938-4246-43.3.331

Chen, I., Hill, J., Ohlemuller, R., Roy, D., & Thomas, C. (2011). Rapid range shifts of species associated with high levels of climate warming. *Science, 333*(6045), 1024-1026. doi: 10.1126/science.1206432

Danby, R., Koh, S., Hik, D. and Price, L. (2011). Four decades of plant community change in the alpine tundra of Southwest Yukon, Canada. *AMBIO, 40*(6), pp. 660-671. doi: 10.1007/s13280-011-0172-2

DiNunzio, M.G. (1972). *A vegetational survey of the alpine zone of the Adirondack Mountains, New York*. M.Sc. Thesis. State University College of Forestry at Syracuse University.

Dirnböck, T., Dullinger, S., & Grabherr, G. (2003). A regional impact assessment of climate and land-use change on alpine vegetation. *Journal of Biogeography, 30*(3), 401-417. doi: 10.1046/j.1365-2699.2003.00839.x

Elith, J., Graham, C. H., Anderson, R. P., Dudı´k, M., Ferrier, S., Guisan, A., … Zimmermann, N. E. (2006). Novel methods improve prediction of species' distributions from occurrence data. *Ecography, 29*, 129-151.

Fick, S., & Hijmans, R. (2017). Worldclim 2: New 1-km spatial resolution climate surfaces for global land areas. *International Journal of Climatology 37,* 4302-4315.

Gabriel H., Talbot S. (1984). *Glossary of landscape and vegetation ecology of Alaska, U.S.* Department of the Interior, Bureau of Land Management, Alaska (1984). Available at: https://www.blm.gov/download/file/fid/22170

Gottfried, M., Pauli, H., Futschik, A., Akhalkatsi, M., Barančok, P., & Benito Alonso, J…. Grabherr, G. (2012). Continent-wide response of mountain vegetation to climate change. *Nature Climate Change, 2*(2), 111-115. doi: 10.1038/nclimate1329

IPCC (2007). *Climate change 2007: Synthesis report. Contribution of working groups I, II and III to the Fourth Assessment Report of the Intergovernmental Panel on Climate Change* [Core Writing Team, Pachauri, R.K and Reisinger, A. (eds.)]. IPCC, Geneva, Switzerland, 104 pp.

Jacobs, J., Chan, S., & Sutton, E. (2014). Climatology of the Forest-Tundra Ecotone at a Maritime Subarctic-Alpine site, Mealy Mountains, Labrador. *ARCTIC, 67*(1), 28. doi: 10.14430/arctic4358

Kimball, K. D., & Weihrauch, D. M., (2000). Alpine vegetation communities and the alpine-treeline ecotone boundary in New England as biomonitors for climate change. *USDA Forest Service Proceedings, 3*(5), 93–101.

Körner, C. (1995). Alpine plant diversity: A global survey and functional interpretations. In: F.S. Chapin & C. Körner (Eds.), *Arctic and Alpine Biodiversity: Patterns, Causes and Ecosystem Consequences.* (Ecological Studies [Analysis and Synthesis], vol. 113). Springer, Berlin, Heidelberg. doi: 10.1007/978-3-642-78966-3_4

Körner, C. (1998). A re-assessment of high elevation treeline positions and their explanation. *Oecologia, 115*(4), 445-459. doi: 10.1007/s004420050540

Körner, C. (2003). *Alpine plant life* (2nd ed., pp. 1-10, 21-26, 77-90). Berlin: Springer Berlin.

Körner, C., & Paulsen, J. (2004). A world-wide study of high altitude treeline temperatures. *Journal of Biogeography, 31*, 713–732.

Körner, C. (2007). Climatic treelines: Conventions, global patterns, causes. *Erdkunde, 61*(4), 316-324. doi: 10.3112/erdkunde.2007.04.02

Minder, J., Mote, P., & Lundquist, J. (2010). Surface temperature lapse rates over complex terrain: Lessons from the Cascade Mountains. *Journal of Geophysical Research, 115*(D14). doi: 10.1029/2009jd013493

Pauli, H., M. Gottfried, and G. Grabherr. (1996). Effects of climate change on mountain ecosystems, upward shifting of alpine plants. *World Resource Review 8*, 382–390.

Paulsen, J., & Körner, C. (2014). A climate-based model to predict potential treeline position around the globe. *Alpine Botany*, *124*(1), 1-12. doi: 10.1007/s00035-014-0124-0

Pepin N., Bradley R., Diaz H., Baraer M., Caceres E., Forsythe N., …Yang, D. Q. (2015). Elevation-dependent warming in mountain regions of the world. *Nature Climate Change, 5*(5), 424-430. doi: 10.1038/nclimate2563

Phillips, S., Dudik, M., & Schapire, R. (2004). A maximum entropy approach to species distribution modeling. *Proceedings of the Twenty-First International Conference on Machine Learning*, 655-662. http://rob.schapire.net/papers/maxent_icml.pdf

Phillips, S., & Dudík, M. (2008). Modeling of species distributions with Maxent: New extensions and a comprehensive evaluation. *Ecography*, *31*(2), 161-175. doi: 10.1111/j.09067590.2008.5203.x

Phillips, S., Anderson, R., Dudík, M., Schapire, R., & Blair, M. (2017). Opening the black box: An open-source release of Maxent. *Ecography, 40*(7), 887-893. doi: 10.1111/ecog.03049

Phillips, S., Anderson, R., Dudík, M & Schapire, R. (2017a). *Maxent software for modeling species niches and distributions* (Version 3.4.1). Available from http://biodiversityinformatics.amnh.org/open_source/maxent/. Accessed on 2019-4-06

Phillips, S. J. (2017b). *A brief tutorial on Maxent*. Retrieved from http://biodiversityinformatics.amnh.org/open_source/maxent/

Robinson, S., Ketchledge, E., Fitzgerald, B., Raynal, D., & Kimmerer, R. (2010). A 23-year assessment of vegetation composition and change in the Adirondack alpine zone, New York State. *Rhodora, 112*(952), 355-377. doi: 10.3119/09-03.1

Rundel, P., & Millar, C. (2016). Alpine ecosystems. In E. Zavaleta & H. Mooney, H. (Eds.), *Ecosystems of California* (pp. 613-634, Chapter 29). Berkeley, California: University of California Press. Available at: https://www.fs.usda.gov/treesearch/pubs/52156

Scherrer, D., & Körner, C. (2010). Infra-red thermometry of alpine landscapes challenges climatic warming projections. *Global Change Biology*, *16*, 2602–2613.

Silva, L., Sun, G., Zhu-Barker, X., Liang, Q., Wu, N., & Horwath, W. (2016). Tree growth acceleration and expansion of alpine forests: The synergistic effect of atmospheric and edaphic change. *Science Advances*, *2*(8), e1501302. doi: 10.1126/sciadv.1501302

Swets, J.A. (1988). Measuring the accuracy of diagnostic systems. *Science*, *240*, 1285–1293.

Natural Resources Canada. (2017). *Canada's plant hardiness site*. Retrieved from: http://planthardiness.gc.ca

PRISM Climate Group, Oregon State U (2015). Retrieved from: http://www.prism.oregonstate.edu/normals

Grabherr, G., Gottfried, M., & Pauli, H. (1994). Climate effects on mountain plants. *Nature, 369*(6480), 448-448. doi: 10.1038/369448a0

United States Geological Survey. (2012). *Bioclimatic predictors for supporting ecological applications in the conterminous United States* (pp. 1-10). Reston, Virginia.

USGCRP (2017). *Climate science special report: Fourth national climate assessment, Volume I* [Wuebbles, D.J., D.W. Fahey, K.A. Hibbard, D.J. Dokken, B.C. Stewart, and T.K. Maycock (eds.)]. U.S. Global Change Research Program, Washington, DC, USA, 470 pp. doi: 10.7930/J0J964J6.

Wiens, J., Stralberg, D., Jongsomjit, D., Howell, C., & Snyder, M. (2009). Niches, models, and climate change: Assessing the assumptions and uncertainties. *Proceedings of the National Academy of Sciences, 106*(Supplement_2), 19729-19736. doi: 10.1073/pnas.0901639106

Wilson, S., & Nilsson C. (2009). Arctic alpine vegetation change over 20 years. *Global Change Biology, 15*, 1676–1684.

TNM Download (2019). Nationalmap.gov. Retrieved from: https://viewer.nationalmap.gov/basic

Zhang, Y., Peterman, M., Aun, D. and Zhang, Y. (2008). Cellular automata: simulating alpine tundra vegetation dynamics in response to global warming. *Arctic, Antarctic, and Alpine Research, 40*(1), 256-263.

Tables

Table 1.)

Feature Types and Associated Statistics Used in Final Maxent Model		
Feature Type	**Calculation Method**	**Associated Statistic**
Raw	Untransformed data	Mean
Quadratic	Square of data values	Variance
Product	Product of two variables	Covariance
Threshold	Transform feature into piecewise function	Min, or Max value
Hinge	Transform feature into linear piecewise function	Min, or Max value

Table 1.) Maxent Feature types along with their method of calculation and the statistic that Maxent calculates using the feature.

Table 2.)

USGS Data Series 691 Bioclimatic Predictor Name-Number Reference		
Predictor Number	**Predictor Name**	**Predictor Units**
BioClim # 1	Annual Mean Temperature	Degrees Celsius
BioClim # 2	Annual Mean Diurnal Range	Degrees Celsius
BioClim # 3	Isothermality	Percent
BioClim # 4	Temperature Seasonality (Standard Deviation)	Degrees Celsius
BioClim # 4a (5)	Temperature Seasonality (CV)	Percent
BioClim # 5 (6)	Max Temperature of Warmest Month	Degrees Celsius
BioClim # 6 (7)	Min Temperature of Coldest Month	Degrees Celsius
BioClim # 7 (8)	Annual Temperature Range	Degrees Celsius
BioClim # 8 (9)	Mean Temperature of Wettest Quarter	Degrees Celsius
BioClim # 9 (10)	Mean Temperature of Driest Quarter	Degrees Celsius
BioClim # 10 (11)	Mean Temperature of Warmest Quarter	Degrees Celsius
BioClim # 11 (12)	Mean Temperature of Coldest Quarter	Degrees Celsius
BioClim # 12 (13)	Annual Precipitation	Millimeters
BioClim # 13 (14)	Precipitation of Wettest Month	Millimeters
BioClim # 14 (15)	Precipitation of Driest Month	Millimeters
BioClim # 15 (16)	Precipitation Seasonality (CV)	Percent
BioClim # 16 (17)	Precipitation of Wettest Quarter	Millimeters
BioClim # 17 (18)	Precipitation of Driest Quarter	Millimeters
BioClim # 18 (19)	Precipitation of Warmest Quarter	Millimeters
BioClim # 19 (20)	Precipitation of Coldest Quarter	Millimeters
Note: Numbers in parenthesis represent alterations to the numbering system that were made for simplifying the raster iteration process in ArcMap. This numbering nomenclature is maintained through all analysis with USGS Bioclim Predictors in this paper.		

Table 2.) USGS Bioclimatic predictor names along with their identification numbers and units

Table 3.)

Results of Linear Regression of Bioclimatic Predictors

Predictor Number	**Predictor Name**	**R^2 Value**	**Lapse Rate (Units/km)**	**Predictor Units**
BioClim # 1	Annual Mean Temperature	0.845	4.794	Degrees Celsius
BioClim # 2	Annual Mean Diurnal Range	0.112	-1.306	Degrees Celsius
BioClim # 3	Isothermality	0.314	-0.457	Percent
BioClim # 4	Temperature Seasonality (Standard Deviation)	0.356	0.758	Degrees Celsius
BioClim # 4a (5)	Temperature Seasonality (CV)	0.156	9.141	Percent
BioClim # 5 (6)	Max Temperature of Warmest Month	0.875	5.435	Degrees Celsius
BioClim # 6 (7)	Min Temperature of Coldest Month	0.406	3.584	Degrees Celsius
BioClim # 7 (8)	Annual Temperature Range	0.140	1.850	Degrees Celsius
BioClim # 8 (9)	Mean Temperature of Wettest Quarter	0.156	4.914	Degrees Celsius
BioClim # 9 (10)	Mean Temperature of Driest Quarter	0.005	4.9111	Degrees Celsius
BioClim # 10 (11)	Mean Temperature of Warmest Quarter	0.911	5.834	Degrees Celsius
BioClim # 11 (12)	Mean Temperature of Coldest Quarter	0.586	3.561	Degrees Celsius
BioClim # 12 (13)	Annual Precipitation	0.398	-442.05	Millimeters
BioClim # 13 (14)	Precipitation of Wettest Month	0.332	-38.42	Millimeters
BioClim # 14 (15)	Precipitation of Driest Month	0.301	-32.35	Millimeters
BioClim # 15 (16)	Precipitation Seasonality (CV)	0.032	3.251	Percent
BioClim # 16 (17)	Precipitation of Wettest Quarter	0.499	-116.07	Millimeters
BioClim # 17 (18)	Precipitation of Driest Quarter	0.269	-106.42	Millimeters
BioClim # 18 (19)	Precipitation of Warmest Quarter	0.528	-99.67	Millimeters
BioClim # 19 (20)	Precipitation of Coldest Quarter	0.289	-125.90	Millimeters

Table 3.) Lapse rates and R^2 values from linear regression of USGS Bioclim variables.

Table 4.)

List of DEMs Used
DEM Name
USGS NED 1/3 arc-second n45w075 1 x 1 degree ArcGrid 2018
USGS NED 1/3 arc-second n44w075 1 x 1 degree ArcGrid 2013
USGS NED 1/3 arc-second n45w074 1 x 1 degree ArcGrid 2018
USGS NED 1/3 arc-second n44w074 1 x 1 degree ArcGrid 2018

Table 4.) List of DEMs used in downscaling analysis and aspect calculation

Table 5.)

Results of Linear Regression of Monthly PRISM Data				
	Precipitation		Temperature	
Month	**R^2 Value**	**Lapse Rate (mm/km)**	**R^2 Value**	**Lapse rate (C/km)**
January	0.373	51.25	0.626	3.610
February	0.392	37.18	0.621	3.530
March	0.227	35.98	0.742	4.644
April	0.353	38.82	0.874	5.195
May	0.472	48.68	0.892	5.332
June	0.578	38.47	0.920	5.674
July	0.547	40.22	0.911	6.031
August	0.476	41.19	0.908	5.416
September	0.597	53.28	0.891	4.847
October	0.686	56.79	0.883	4.216
November	0.537	53.61	0.892	4.642
December	0.453	52.64	0.816	4.493

Table 5.) Lapse rates and r^2 values for linear regression of PRISM monthly data

Table 6.)

Maxent Model Run Settings and Data					
Model Run Reference	**Environmental Dataset; Resolution**	**Analysis Region**	**Number of Presence Points**	**Percent of Points Used for Training**	**Projection Onto Future Climate Performed**
BC-1	All 20 USGS Bioclim Predictors; 400m	Lat (43.2, 44.95) Lon (-75.0,-73.4)	100	25	No
TPA-1	Annual Mean Temp, Annual Mean Precip, Non-Masked Aspect; 10m	Lat (43.3, 48.8) Lon (-74.85, -73.45)	2500	25	No
TPA-2	Annual Mean Temp, Annual Mean Precip, Masked Aspect; 10m	Lat (43.3, 48.8) Lon (-74.85, -73.45)	2500	25	No
TP-1	Annual Mean Temp, Annual Mean Precip; 10m	Lat (43.3, 48.8) Lon (-74.85, -73.45)	2500	25	No
Note: All settings not listed were kept at the default values for Maxent version 3.4.1					

Table 6.) Information on the parameters and settings used in each of the Maxent models run in this project

Table 7.)

Model Run AUC Values	
BC-1	0.998
TP-1	0.996
TPA-1	0.995
TPA-2	0.995

Table 7.) The AUC values generated by Maxent for each of the model runs

Table 8.)

Analysis of Variable Contributions in USGS Bioclimatic Variable Maxent Run

Variable	Percent contribution	Permutation importance
band12	79.7	0
band10	12.8	0
band1	2.3	2.1
band11	2.2	0
band7	1.1	83.5
band16	1.1	13.1
band5	0.7	0
band3	0.1	1.3
band6	0.1	0

Table 8: Analysis of variable contributions from the variables that contributed to Maxent model skill. This run used USGS Bioclimatic variables as environmental input. Variables with values of zero for both percent contribution and permutation importance are not included.

Table 9.)

Lambdas File Output for TP-1			
Feature Name and Type	**Lambda Value**	**Min Value of Variable in Training**	**Max Value of Variable in Training**
annual average precipitation	0	66.13546753	161.7019958
annual average temperature	0	0.765864909	8.779252052
annual average precipitation ^2	-0.023065336	4373.900065	26147.53546
annual average precipitation*annual average temperature	-0.250583576	123.8378993	792.7650805
annual average temperature – FH	-1.244019818	2.242676973	8.779252052
annual average temperature – FH	-1.872197352	2.448004603	8.779252052
annual average temperature – FH	-2.147196104	2.488901019	8.779252052
annual average temperature – FH	-2.07628575	2.501142979	8.779252052
annual average temperature – FH	-3.561273582	2.504409432	8.779252052
annual average temperature – FH	-0.849498498	2.481745005	8.779252052
annual average precipitation – RH	-0.404996825	66.13546753	125.2432976
annual average precipitation – RH	-0.715324481	66.13546753	125.2659988
annual average temperature – FH	-0.423241992	2.447395086	8.779252052
annual average temperature – FH	-0.967791773	2.426437497	8.779252052
Key: Feature name = Raw feature Feature Name*Feature Name = Product Feature ^2 = Quadratic feature - RH = Reverse Hinge feature - FH = Forward Hinge feature (Feature Name = integer) = Threshold feature			

Table 9.) Content of lambdas file for model TP-1

Table 10.)

Lambdas File Output for TPA-1			
Feature Name and Type	**Lambda Value**	**Min Value of Variable in Training**	**Max Value of Variable in Training**
(aspect=0.0)	0	0	1
(aspect=5.0)	0.005402358	0	1
(aspect=6.0)	0.095019442	0	1
(aspect=7.0)	-0.019238857	0	1
annual average precipitation	0	66.22400665	161.7019958
annual average temperature	-0.187504878	0.76709491	8.784367561
annual average precipitation **^2**	-0.002878165	4385.619057	26147.53546
annual average temperature **^2**	-41.68903447	0.588434601	77.16511345
annual average precipitation*annual average temperature	-1.145853736	124.040778	792.2790877
annual average temperature – FH	-0.857624798	0.76709491	1.746787012
annual average temperature – FH	-0.405721956	0.76709491	1.775585473
annual average temperature – FH	-0.027880508	0.76709491	1.761152983
Key: Feature name = Raw feature Feature Name*Feature Name = Product Feature ^2 = Quadratic feature - RH = Reverse Hinge feature - FH = Forward Hinge feature (Name = integer) = Threshold feature			

Table 10.) Content of lambdas file for model TPA-1

Table 11.)

Lambdas File Output for TPA-2			
Feature Name and Type	**Lambda Value**	**Min Value of Variable in Training**	**Max Value of Variable in Training**
(acpect_masked=1.0)	0	0	1
(acpect_masked=5.0)	0.012163054	0	1
(acpect_masked=6.0)	0.157018512	0	1
annual average precipitation – RH	-0.005055165	66.19568634	161.7019958
annual average temperature – FH	-17.08529721	0.76709491	8.792941093
ann_avg_precip^2	-0.048601349	4381.86889	26147.53546
ann_avg_temp^2	-16.3627547	0.588434601	77.31581307
annual average precipitation*annual average temperature	-0.065374358	124.040778	795.4974585
annual average temperature – FH	-0.138296071	0.76709491	1.727829516
annual average temperature – FH	-1.636171559	0.76709491	1.746787012
annual average temperature – FH	-0.312906592	0.76709491	1.761152983
annual average temperature – FH	-0.045032511	0.76709491	1.775585473
annual average temperature – FH	-0.206389011	0.76709491	1.625766993
Key: Feature name = Raw feature Feature Name*Feature Name = Product Feature ^2 = Quadratic feature - RH = Reverse Hinge feature - FH = Forward Hinge feature (Name = integer) = Threshold feature			

Table 11.) Content of lambdas file for model TPA-2

Figures

Figure 1.)

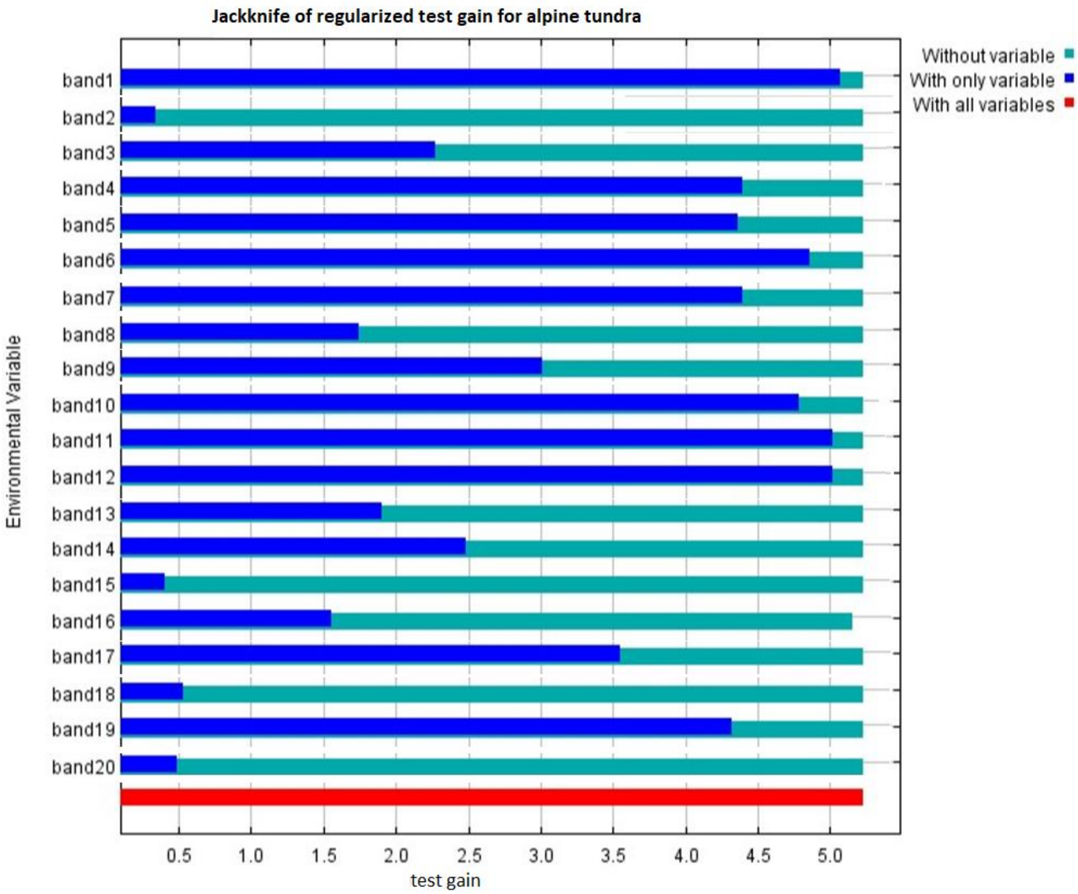

Figure 1.) Results of jackknife analysis from model BC-1

Figure 2.)

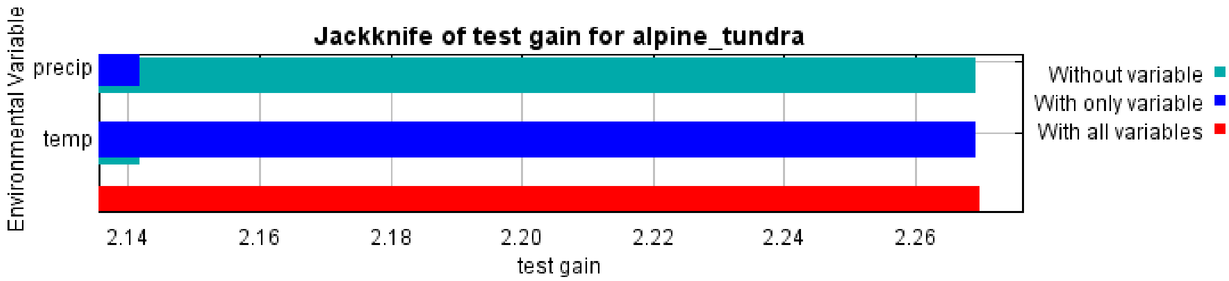

Fig 2.) Maxent output of test gain (a measure of total skill gain) for jackknife analysis from model TP-1

Figure 3.)

TPA-1 Response Histogram

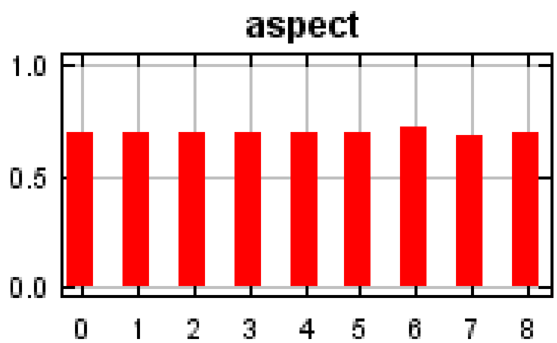

Figure 3.) Response curve for aspect in model TPA-1, the analysis using non-masked aspect. Values of 0 indicate flat ground, values from 1 to 8 indicate 45 degree increments of direction starting at N followed by NE, around to NW at 8

Figure 4.)

TPA-2 Response Histogram

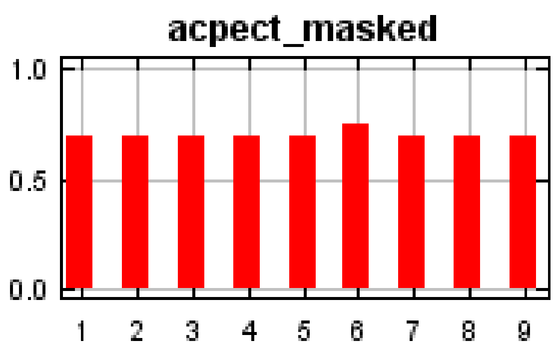

Figure 4.) Response curve for aspect in model TPA-2, the analysis using masked aspect. Values of 0 indicate flat ground, values from 1 to 8 indicate 45 degree increments of direction starting at N followed by NE, around to NW at 8

Figure 5

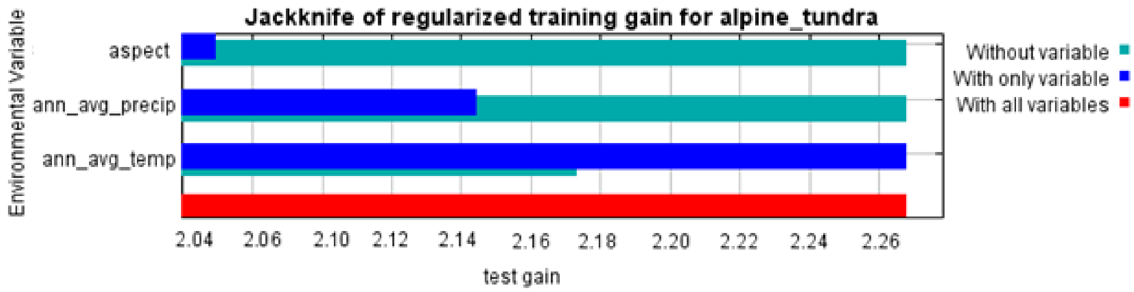

Figure 5.) Jackknife analysis from model with non-masked aspect values.

Figure 6

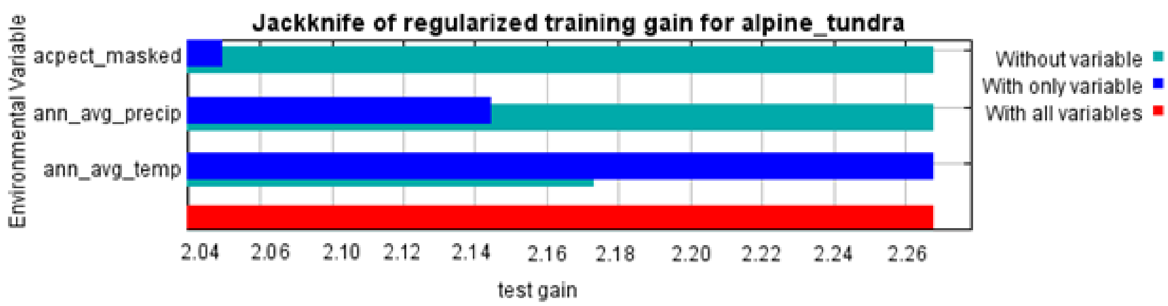

Figure 6.) Jackknife analysis from model with masked aspect values.

Figure 7.)

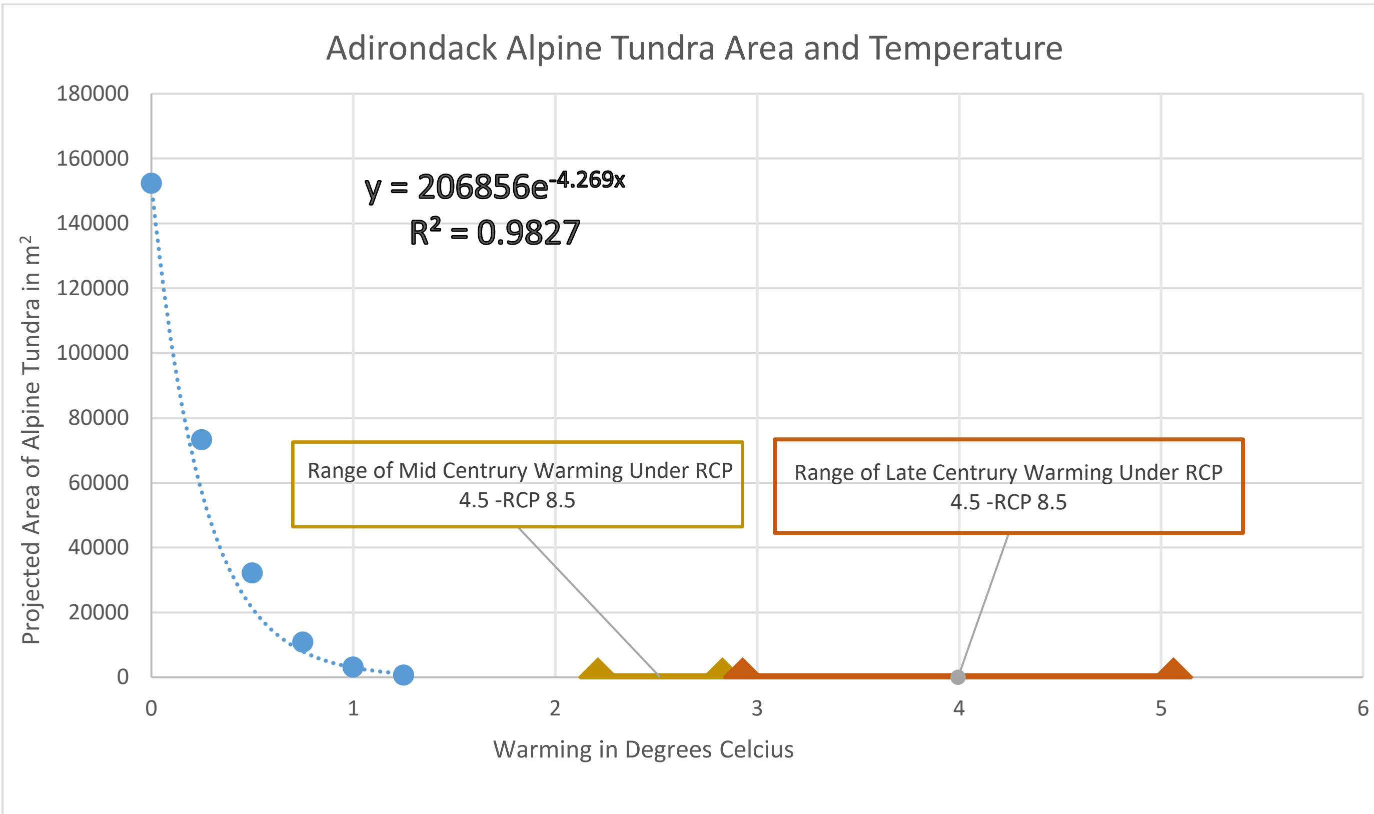

Figure 7.) Predicted alpine tundra area at various amounts of warming along with Mid-Century and Late Century estimates of warming based on RCP 4.5 and 8.5 over the Northeast United States. The dotted line depicts the line of best fit for the alpine tundra area data. The two colored lines on the X axis depict the range of projected warming in the Northeast United States between climate scenarios RCP 4.5 and RCP 8.5 at two different future times.

Figure 8.)

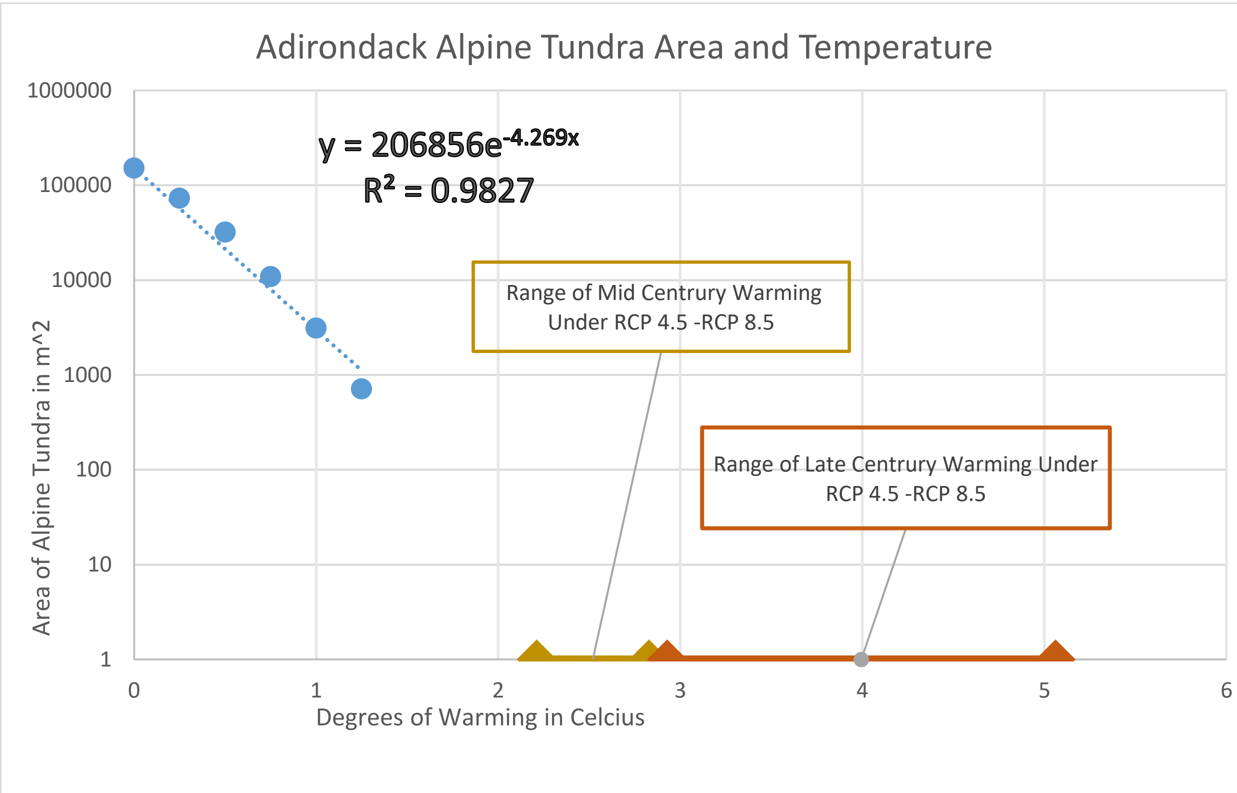

Figure 8.) Predicted alpine tundra area at various amounts of warming along with Mid-Century and Late Century estimates of warming based on RCP 4.5 and 8.5 over the Northeast United States plotted on a logarithmic scale. The dotted line depicts the line of best fit for the alpine tundra area data. The two colored lines on the X axis depict the range of projected warming in the Northeast United States between climate scenarios RCP 4.5 and RCP 8.5 at two different future times.